Swelling Kinetic Study and Characterization of Crosslinked Hydrogels Containing Silver Nanoparticles

Enas M. Ahmed, Fatma S. Aggor

Chemical Engineering and Pilot Plant Department, Engineering Research Division, National Research Centre, Dokki, Cairo, Egypt

Received 8 July 2008; accepted 28 November 2009
DOI 10.1002/app.31934
Published online 7 April 2010 in Wiley InterScience (www.interscience.wiley.com).

ABSTRACT: The ammonium persulfate induced polymerization of acrylamide in the presence of silver nitrate ($AgNO_3$) and *N*,*N*′-methylenebisacrylamide as a crosslinking agent were used to prepare crosslinked hydrogels containing silver ions. Subjecting this hydrogel to reduction with sodium hydroxide brought to focus the nanosilver hydrogel composites. Characterization of the latter, including proof of existence of silver nanoparticles in the hydrogel, was made. The number of silver nanoparticles embedded in the hydrogel matrix was higher at higher concentration of $AgNO_3$ used in the preparation of the nanosilver hydrogel composite. The characterization was performed by the use of ultraviolet–visible spectroscopy and transmission electron microscopy. The swellability of the hydrogel containing nanosilver particles was also studied, and the dependence of the swellability on the abundance of silver nanoparticles in the hydrogel composite was verified. It was further disclosed that the kinetic model matched the experimental data; meanwhile, the diffusion of water into the hydrogel was non-Fickian type. © 2010 Wiley Periodicals, Inc. J Appl Polym Sci 117: 2168–2174, 2010

Key words: crosslinking; hydrogels; kinetics (polym.)

INTRODUCTION

Hydrogels are insoluble polymeric materials containing a large number of hydrophilic groups capable of holding a large amount of water in their three-dimensional networks. Over the past 3 decades, a number of hydrogels differing in structure, composition, and properties have been developed. Hydrogel networks can be formed by conventional crosslinking methods or free-radical polymerization processes initiated by thermal and redox systems or by the use of free-radical initiators activated by irradiation in the form of E-beams, microwaves, γ rays, or light, including UV, visible, or near infrared light.[1] Because of their biocompatibility, permeability, and physical characteristics, hydrogels are suitable for use in many agricultural, industrial, and medical applications.[2–6] Moreover, the development of nanoparticles and nanostructural materials have opened a new era for the construction of well-designed nanostructures, which have been considered a novel class of materials for catalytic, optical, electronic, and biomedical applications.[7]

Correspondence to: E. M. Ahmed (elarefenas123@yahoo.com).

Journal of Applied Polymer Science, Vol. 117, 2168–2174 (2010)

Recently, much research and development efforts have been devoted to the production of hydrogels containing metal nanoparticles, as these hydrogels find enormous valuable applications in biorelated fields.[8] Nanomaterials have a comparatively wider surface area than an equal weight of the same material in large form. This leads to higher chemical and physical activity. In addition, materials with nanosizes of less than 50 nm exhibit quantum effects on optical, electrical, and magnetic characteristics different from those with large particles.[9] So they will play an important roles in the future because of their unique biological, chemical, and physical properties. Nanosilver particles have been applied to a wide range of healthcare products, including burn dressings, scaffolds, skin donor and recipient sites, water purification systems, and medical devices.[10–12]

Hydrogel composites containing bearing metal nanoparticles have attracted much attention because of their unique optical, electrical, and catalytic behaviors.[12,13] Pardo-Yissar et al.[14] prepared crosslinked polyacrylamide (PAAm) hydrogels by the electropolymerization of acrylamide monomer (AAm) on Au-wire electrodes in the presence of a crosslinker. A few studies have dealt with hydrogels containing metal nanoparticles; for example, hydrogels containing silver, gold, and copper have exhibited resistance to microorganisms.[15–18] Among these nanoparticles, nanosilver has displayed acceptable antimicrobial properties.[19–21] Nanosilver particles

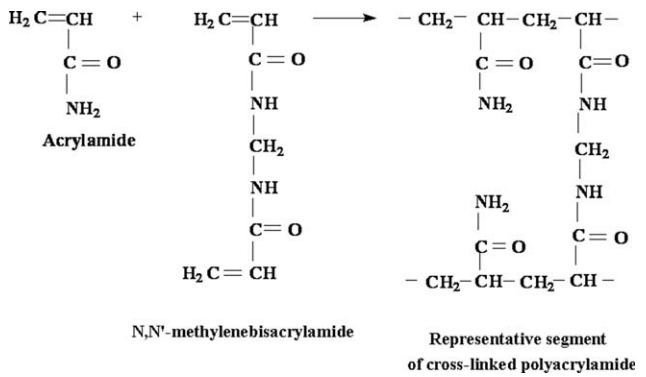

Figure 1 Polymerization of AAm.

have been introduced to a wide range of medical applications and water-purifying systems.[8,10,12]

Saravanan et al.[22] showed that the use of PAAm hydrogels was effective for the production of silver nanoparticles. Previous reports also described the preparation of nanosilver hydrogel composites via the gelation of physically combined separately prepared nanoparticles and hydrogel composites.[23]

Furthermore, a series of antibacterial superabsorbents containing silver hydrogel nanocomposites were successfully prepared by inverse suspension polymerization.[23]

Silver nanoparticles proved to be nontoxic and ecofriendly antibacterial agents. The problem of silver's weak binding properties was overcome via the preparation of stabilized polymer nanoparticles, which were embedded in hydrogel networks.[24–29]

In this study, we aimed to prepare and characterize crosslinked PAAm hydrogels containing silver nanoparticles (Ag/PAAm). The preparation of such Ag/PAAm composites was performed through the free-radical polymerization of AAm intercalated in a silver nitrate ($AgNO_3$) solution in the presence of crosslinker. After reduction, the obtained composite was characterized itself with ultraviolet–visible spectroscopy and transmission electron microscopy (TEM). The study was extended to include a intensive kinetic study of the swellability of the nanosilver–hydrogel composites and the dependence of the swellability on the amount of silver nanoparticles in the composites.

Generally, PAAm gels result from polymerization of AAm with a suitable bifunctional crosslinking agent, most commonly, *N,N′*-methylenebisacrylamide (MBAm; Fig. 1). Gel polymerization is usually initiated with ammonium persulfate (APS).

EXPERIMENTAL

Materials

AAm was provided by Sisco Research Laboratory PVT., Ltd. (Mumbai, India); MBAm, APS, and $AgNO_3$ were supplied by Sigma-Aldrich, Inc., and sodium hydroxide (NaOH) pellets (99%) were purchased from Modern Laboratory (Egypt). These reagents were used as laboratory-grade chemicals.

Synthesis of crosslinked PAAm hydrogels containing silver nanoparticles

The preparation of crosslinked PAAm hydrogels containing nanosized silver particles was carried out according to a reported procedure.[21] A weighed amount of $AgNO_3$ was dissolved in double-distilled water, and desired amounts of AAm and MBAm were added under mechanical stirring and a nitrogen atmosphere. The mixture was heated gently up to 70°C, and a catalytic amount of APS was added under continuous stirring for 30 min; the mixture was then washed thoroughly with double-distilled water. The resulting hydrogel was then added to an aqueous solution of NaOH (5 wt %), and the reaction was allowed to proceed overnight until the complete reduction of Ag^+ ions occurred. This was indicated by a faint yellow color in the colloidal Ag nanoparticles within the hydrogel network. The hydrogel was then washed several times in double-distilled water and kept until complete swelling occurred.

A blank experiment (where Ag^+ ions were omitted) was also conducted. The preparation of Ag/PAAm hydrogels with different molar ratios of AAm/Ag^+ ions was also conducted. The prepared hydrogels were air-dried and then vacuum-died and then kept for characterization. All of the experiments were duplicated to obtain average results.

Characterization

The ultraviolet–visible spectra of the nanosilver hydrogel composites were taken on a Jenway spectrophotometer (model 6310; Bibby Scientific Ltd., Dunmow, Essex, UK).

TEM images for the blank hydrogel and nanosilver hydrogel composites were recorded with a JEOL JEM-1230 electron microscope operating at an acceleration voltage of 100 kV. Specimens for TEM were prepared by the placement of a swelled sample of hydrogel on a 400-mesh copper grid and the evaporation of excess water in air at room temperature (25 ± 1°C).

Swelling studies

The swelling properties of the blank hydrogel and nanosilver hydrogel composites, such as the swelling ratio (S) and equilibrium swelling ratio (S_{eq}), were determined with the conventional gravimetric method and calculated with the following equations:[30]

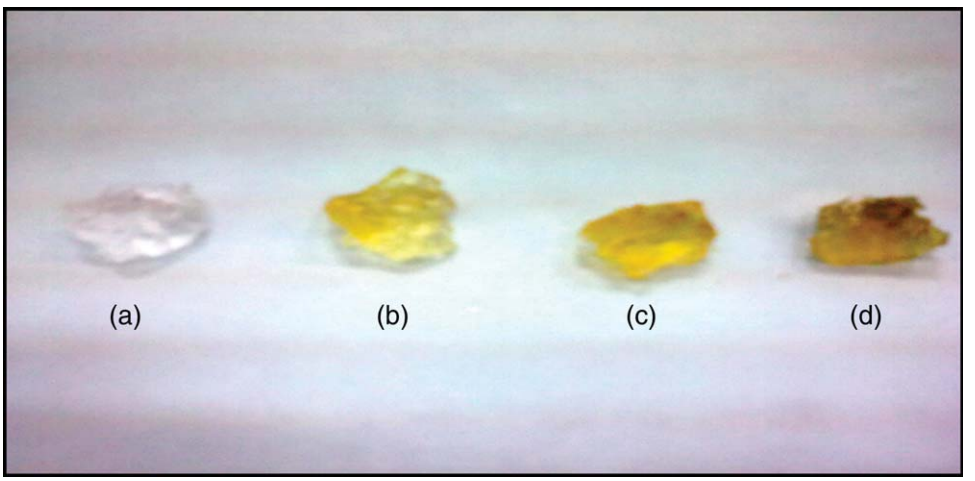

Figure 2 Photographs of the Ag/PAAm hydrogel nanocomposites with different molar ratios of monomer to Ag+ ions: (a) 1 : 0, (b) 1 : 1 × 10^{-3}, (c) 1 : 2 × 10^{-3}, and (d) 1 : 3 × 10^{-3}. [Color figure can be viewed in the online issue, which is available at www.interscience.wiley.com.]

$$S(\mathrm{g/g}) = \frac{(W_t - W_0)}{W_0} \quad (1)$$

$$S_{\mathrm{eq}}(\mathrm{g/g}) = \frac{(W_{\mathrm{eq}} - W_0)}{W_0} \quad (2)$$

where W_0, W_t, and W_{eq} are the weights of the samples in the dry state, the swollen state at a certain time, and the completely (equilibrium) swollen state, respectively.

The equilibrium swelling of the gels was determined as follows: gels were dried for a day at room temperature and were then dried in vacuo at 60°C. After the weight of the dried samples was determined, the samples were equilibrated in distilled water for 3 days at room temperature and then weighed again.

RESULTS AND DISCUSSION

The production of nanoparticles in the hydrogel networks systems was considered as the most important approach because of its direct applicability in various fields of applications. The free network spaces between hydrogel networks reserve and stabilize nanoparticles. Moreover, the *in situ* reduction of metal ions and the stabilization of particles can be clarified by the following: (1) metal ions are attached to reactive sites of hydrogel networks, and larger amounts of metal ions are embedded in the network spaces of hydrogels; (2) the reduction process proceeds under the action of NaOH; and (3) the resulting particles are well stabilized through the hydrogel network interspaces.[31]

The Ag/PAAm hydrogel composites before hydrolysis turned black when stored under normal conditions, whereas the hydrogel composites after hydrolysis and storage for a long time exhibited a faint yellow color. This indicated that the Ag/PAAm hydrogels did not undergo any oxidation and that the Ag^+ ions were completely reduced. This was evidenced by a work published elsewhere.[32]

Figure 2 illustrates the formation of silver nanoparticles embedded in the swollen PAAm hydrogel composites. The formation of the silver nanoparticles in the hydrogel networks was confirmed by the appearance of a yellow color. This was ascribed to the adsorption of silver nanoparticles in the hydrogel matrix. An increase in the silver concentration in the reaction medium led to the appearance of samples with darker color shades.

Absorption properties

Spectral studies were used as a tool to confirm the presence of embedded silver nanoparticles within the hydrogel macromolecular networks. As presented in Figure 3, all of the spectra of silver nanoparticle hydrogel networks showed a distinct characteristic absorption peak around 420 nm. This was a manifestation of the surface plasmon resonance effect of quantum-size silver nanoparticles present in the hydrogel networks. However, the plain PAAm hydrogel did not show any such peak. Murali Mohan et al.[28] produced silver nanoparticles (≈ 3 nm) within poly(*N*-isopropylacrylamide-*co*-sodium acrylate) hydrogels that also showed a well-defined surface plasmon resonance around 400 nm.

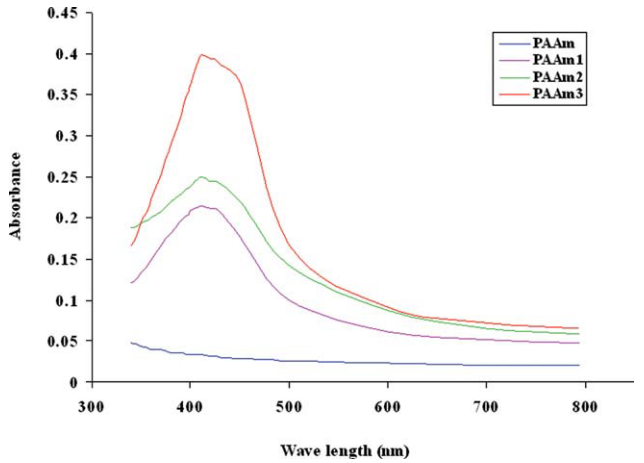

Figure 3 Absorption spectra of the blank PAAm and Ag/PAAm hydrogel nanocomposites corresponding to different molar ratios of monomer to Ag^+ ion PAAm (1 : 0), PAAm1 (1 : 1 × 10^{-3}), PAAm2 (1 : 2 × 10^{-3}), and PAAm3 (1 : 3 × 10^{-3}). [Color figure can be viewed in the online issue, which is available at www.interscience.wiley.com.]

TEM

TEM was used to obtain more information about the size of the silver nanoparticles. Figure 4(a–c) depicts the morphology of nanosilver hydrogel composites obtained with different molar ratios of monomer to Ag^+ ion. Obviously, no silver nanoparticles appeared in the plain sample [Fig. 4(a)], whereas Ag particles were clearly observed in the other two samples [Figs. 4(b,c)].

Figure 5(a,b) shows that the surface plasmon bands displayed a symmetrical configuration and the intensity of the plasmon band increased with increasing Ag^+ ion concentration. In general, the enhancement in the intensity of the absorption band was brought by the increase of the metal particle size in combination with the band shift. The size of the Ag nanoparticles was not altered by the change in the Ag^+ ion concentration, and the enhancement in intensity was due to the larger number of Ag particles formed with the increase in metal precursor

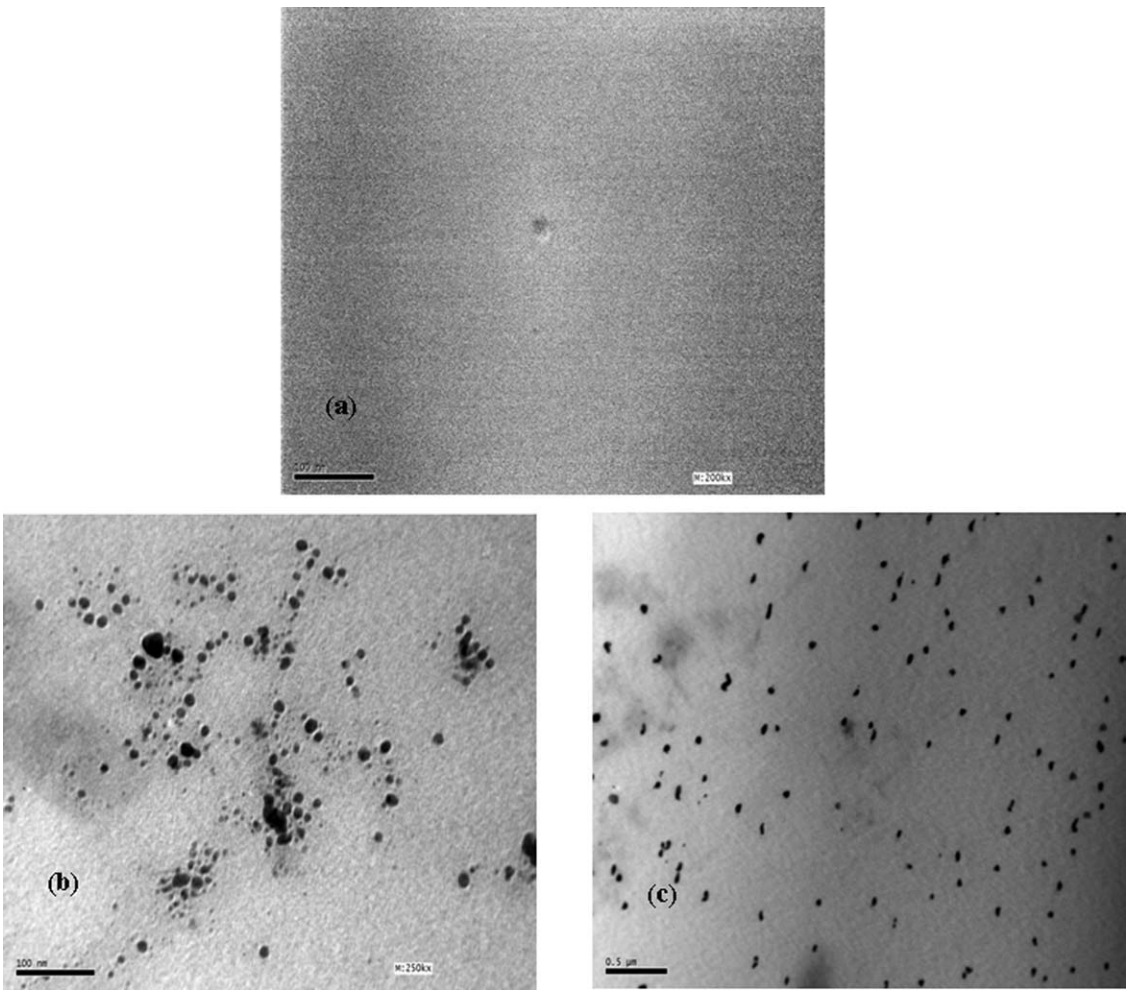

Figure 4 TEM images of the silver nanoparticles obtained from (a) PAAm, (b) Ag/PAAm1, and (c) Ag/PAAm2.

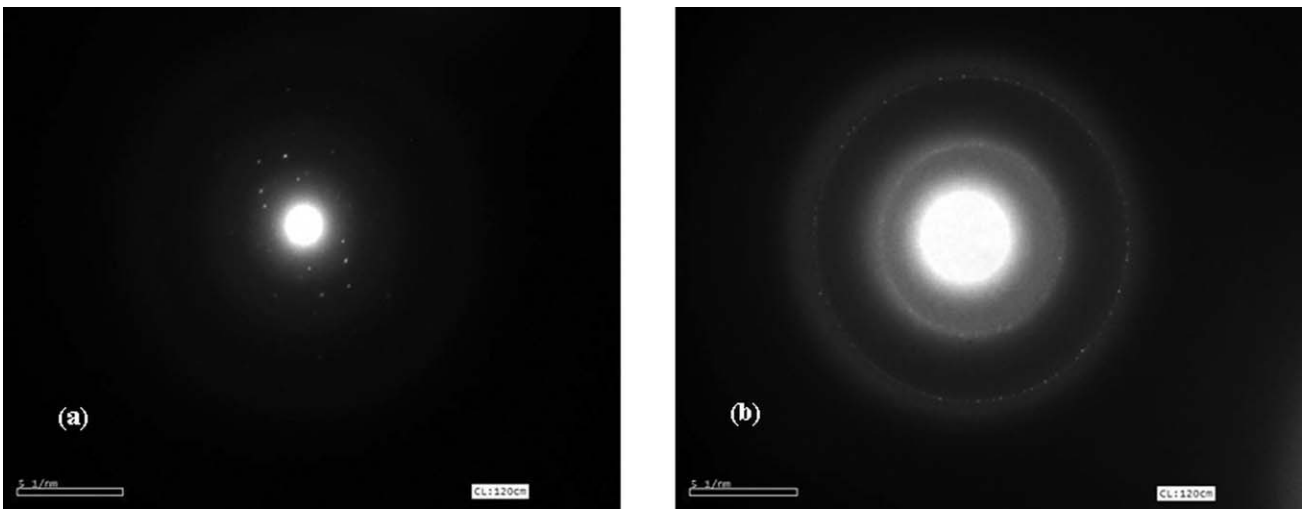

Figure 5 Selected area electron diffraction pattern within (a) Ag/PAAm1 and (b) Ag/PAAm2.

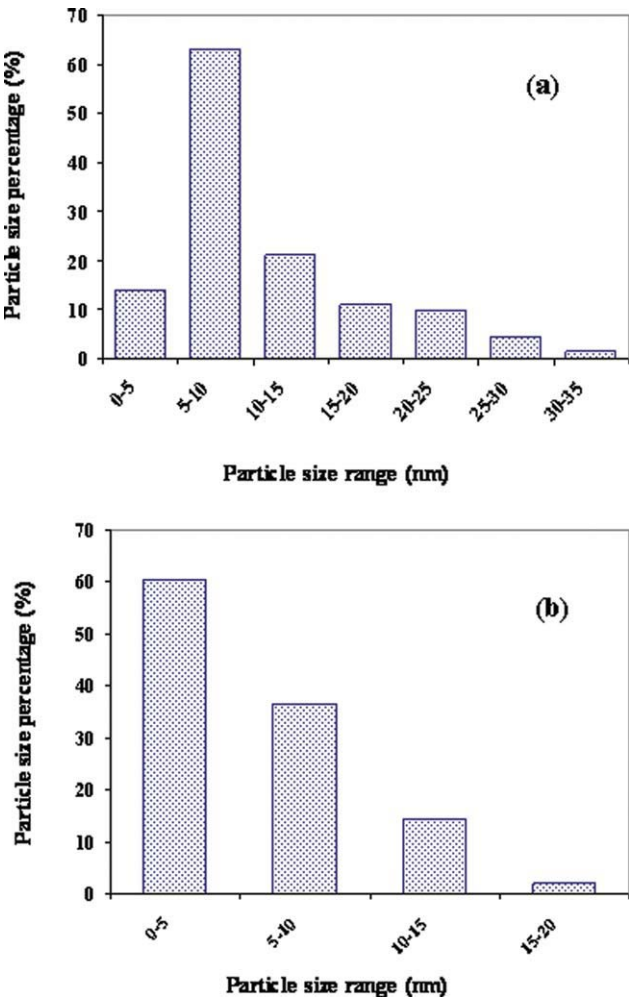

Figure 6 Histogram for the size distribution of Ag nanoparticles within the (a) Ag/PAAm1 and (b) Ag/PAAm2 hydrogel nanocomposites. [Color figure can be viewed in the online issue, which is available at www.interscience.wiley.com.]

concentration. These conclusions were conformed with the TEM results.

The histogram of size distribution derived from the TEM image is shown in Figure 6(a,b). The figure shows that the particle size ranged from 5 to 15 nm, with some particles of 20–25 nm and a small percentage having a diameter of 30–35 nm.

Swelling behavior

Swelling experiments were carried out at room temperature (25 ± 1°C) to evaluate the swelling capacity in distilled water of the hydrogels under investigation. The increase in the weight of the swollen hydrogels was directly related to the time of

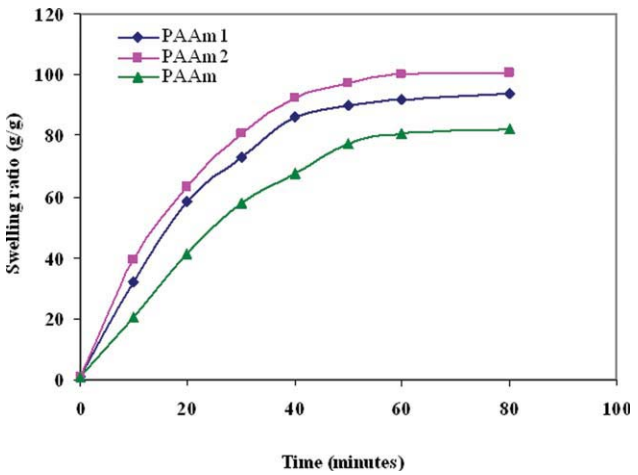

Figure 7 Swelling behavior of the hydrogel nanocomposites and nanosilver hydrogel composites corresponding to different molar ratios of monomer to Ag^+ ions: PAAm (1 : 0), PAAm1 (1 : 1 × 10^{-3}), and PAAm2 (1 : 2 × 10^{-3}). [Color figure can be viewed in the online issue, which is available at www.interscience.wiley.com.]

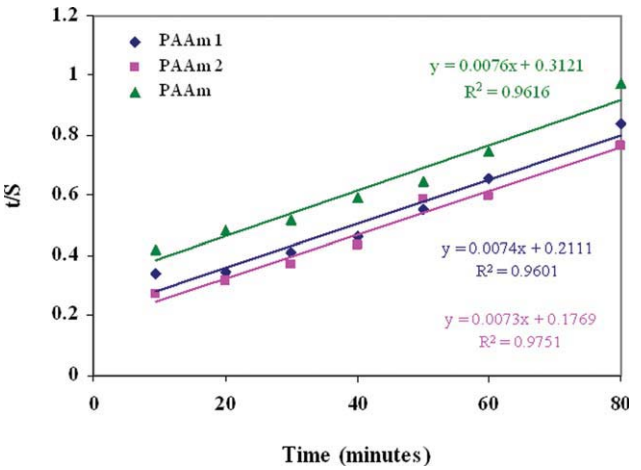

Figure 8 Swelling rate relations of the hydrogels, nanocomposites, and nanosilver–hydrogel composites corresponding to different molar ratios of monomer to Ag^+ ions: PAAm (1 : 0), PAAm1 ($1 : 1 \times 10^{-3}$), and PAAm2 ($1 : 2 \times 10^{-3}$). [Color figure can be viewed in the online issue, which is available at www.interscience.wiley.com.]

swelling. That is, the increase in the weight of the swollen hydrogel increased with increasing time of swelling. The swelling behavior observed was associated with the absorption mechanism, which, in turn, was determined by the diffusion process.

Figure 7 illustrates the effect of the presence of Ag nanoparticles on the swelling characteristics of the hydrogel composites. It was clear that S increased sharply upon prolongation of the swelling time up to about 50 min and then leveled off thereafter. It was also clear that presence of Ag nanoparticles embedded in the hydrogel caused the enlargement of the hydrogel networks. A considerable variation in the swelling capacity of the Ag/PAAm nanocomposite hydrogels was noted when the hydrogels were modified or loaded with Ag nanoparticles. The formed silver nanoparticles with different amounts of Ag nanoparticles inside the gel caused the expansion of the hydrogel networks. The significant increase in the degree of hydration was attributed to the presence of the surface charge of Ag colloidal nanoparticles. Moreover, increasing the amount of Ag nanoparticles enhanced the swellability of the hosting hydrogel nanocomposites and followed the order PAAm2 > PAAm1 > Blank PAAm. These results were in accordance with those of the reports published by Saravanan et al.[22] and Murali Mohan et al.[28]

Swelling kinetic study

The controlling mechanism of the swelling processes was visualized through kinetic models. The latter were used to examine the data derived from the experimental work. A simple kinetic analysis is represented by a second-order equation, as given:[33–35]

$$\frac{dS}{dt} = k_S(S_{eq} - S)^2 \tag{3}$$

where k_s is the swelling rate constant and S_{eq} is the degree of swelling at the state of equilibrium. After integration, when the initial conditions $S = 0$ at $t = 0$ and $S = S$ at $t = t$, were applicable, eq. (3) became as follows:

$$\frac{t}{S} = A + Bt \tag{4}$$

where $B = 1/S_{eq}$ is the inverse of the maximum or equilibrium swelling and $A = 1/k_S S_{eq}^2$ is the reciprocal of the rate of swelling at the initial state $[(dS/dt)_0]$ of the hydrogel. We examined the kinetic models by plotting t/S versus t for PAAm, PAAm1, and PAAm2. The swelling parameters, including initial swelling rate (r), k_S, and maximum equilibrium swelling $[(S_{eq})_{max}]$, were calculated from the equations of the straight lines given in Figure 8. The calculated values are listed in Table I.

The mechanism of water diffusion in swellable polymeric hydrogels has attracted much attention because of its many biomedicine, environmental, pharmaceutical, and agriculture applications. The diffusion of water implied that the hydrogel could be evaluated with the following equation:[36]

$$S(g/g) = \frac{(W_t - W_0)}{W_0} = Kt^n \tag{5}$$

TABLE I
Some Swelling Parameters of PAAm and the Ag/PAAm Hydrogel Nanocomposites

Swelling parameter	Molar ratio of monomer to Ag^+ ions		
	1 : 0	$1 : 0.1 \times 10^{-3}$	$1 : 0.2 \times 10^{-2}$
Experimental equilibrium swelling	82.1	93.63	100.48
$(S_{eq})_{max}$	131.6	135.14	136.99
$k_s \times 10^6$	1.86	2.62	3.05
r	3.20	4.74	5.65
n	0.775	0.59	0.53

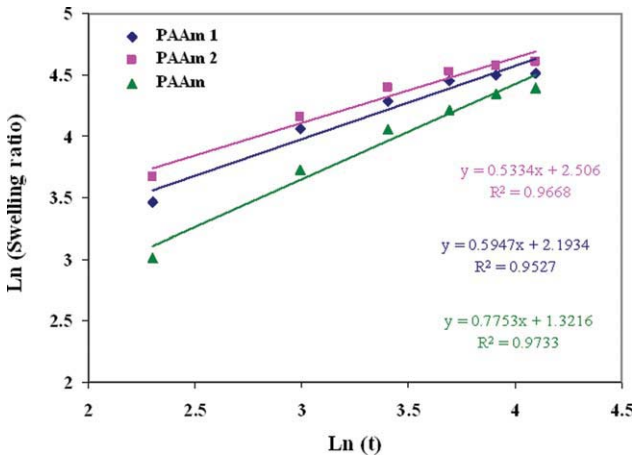

Figure 9 Swelling kinetic relations of the hydrogel nanocomposites and nanosilver–hydrogel composites corresponding to different molar ratios of monomer to Ag^+ ions: PAAm (1 : 0), PAAm1 ($1 : 1 \times 10^{-3}$), and PAAm2 ($1 : 2 \times 10^{-3}$). [Color figure can be viewed in the online issue, which is available at www.interscience.wiley.com.]

where K is the swelling constant and n is the swelling exponent calculated from the slopes of the lines of Ln S versus Ln t plots. For cylindrical shapes, $n =$ 0.45–0.50 and corresponds to Fickian diffusion, whereas $0.50 < n < 1.0$ indicates that the diffusion is non-Fickian type.[36] From Figure 9, the values of n were found to be between 0.53 and 0.775. The values of n indicated that the diffusion was non-Fickian type. Values of n lying between 0.5 and 1 indicated anomalous diffusion.[37]

CONCLUSIONS

Nanosilver crosslinked polyamide hydrogel composites (Ag/PAAm) were prepared through the free-radical polymerization of AAm with APS in the presence of $AgNO_3$ and MBAm as a crosslinker. The reduction of Ag^+ intercalated in the hydrogel composites to Ag metal was effected by NaOH. Characterization of the resulting composites confirmed that they exhibited a surface plasmon band around 420 nm for the existence of Ag nanoparticles within the hydrogels.

TEM micrographs revealed the presence of Ag nanoparticles within the hydrogel matrix and the number of nanoparticles increased at higher concentration of Ag^+ ions. The swellability of Ag/PAAm was dependent on the abundance of silver nanoparticles in the PAAm hydrogels and followed the order: Ag/PAAm2 > Ag/PAAm1 > Blank. The swelling kinetic model was found to be in agreement with experimental data, and the diffusion of water into the hydrogels was the non-Fickian type.

The authors thank Hala A. Talaat, Professor of Chemical Engineering, National Research Centre, Egypt, for her kind support and for help with the electron microscopic analysis in this study.

References

1. Abdel-Aal, S. E.; Gad, Y. H.; Dessouki, A. M. J Hazard Mater B 2006, 129, 204.
2. Laurence, M. M.; Thomas, L. M.; Pierre, E. B.; Dominique, P. P.; Ralph, M.; Jan-Anders, E. M. Biomaterials 2006, 27, 905.
3. Elvira, C.; Mano, J. F.; San Román, J.; Reis, R. L. Biomaterials 2002, 23, 1955.
4. Hoch, G.; Chauhan, A.; Radke, C. J. J Membr Sci 2003, 214, 199.
5. Ghanshyam, S. C.; Baljit, S.; Sandeep, C.; Monica, V.; Swati, M. Desalination 2005, 181, 217.
6. Huarong, N.; Mingzhu, L.; Falu, Z.; Mingyu, G. Polymers 2004, 58, 185.
7. Dutta, J.; Hofmann, H. In: Encyclopedia of Nanoscience and Nanotechnology; Nalwa, H. S., Ed.; Vol 9, American Scientific Publishers, 2004, p 617.
8. Thomas, V.; Yallapu, M. M.; Sreedhar, B.; Bajpai, S. K. J Colloid Interface Sci 2007, 315, 389.
9. Mohanpuria, P.; Nisha, K.; Sudesh, R.; Yadav, K. J Nanopart Res 2008, 10, 507.
10. Jain, P.; Pradeep, T. Biotechnol Bioeng 2005, 90, 59.
11. Sondi, I.; Salopek-Sondi, B. J Colloid Interface Sci 2004, 275, 177.
12. Zuhuang, J. Chin. Pat. CN 1387700 (2003).
13. Shipway, A. N.; Willner, I. Chem Commun 2001, 20, 35.
14. Pardo-Yissar, V.; Gabai, R.; Shipway, A. N.; Bourenko, T.; Willner, I. Adv Mater 2001, 13, 1320.
15. Feng, Q. L.; Cui, F. Z.; Kim, T. N.; Kim, J. W. J Mater Sci Lett 1999, 18, 559.
16. Silver, S. FEMS Microbiol Rev 2003, 27, 341.
17. Yeo, S. Y.; Jeong, S. H. Polym Int 2003, 52, 1053.
18. Lee, H. J.; Yeo, S. Y.; Jeong, S. H. J Mater Sci 2003, 38, 2199.
19. Margaret, I.; Lui, S. L.; Poon, V. K. M.; Lung, I.; Burd, A. J Med Microbiol 2006, 55, 59.
20. Maki, D. G.; Tambyah, P. A. Emerg Infect Dis 2001, 7, 342.
21. Curtin, J. J.; Donlan, M. R. Agents Chemother 2006, 50, 1268.
22. Saravanan, P.; Padmanabha Raju, M.; Alam, S. Mater Chem Phys 2007, 103, 278.
23. Lee, W. F.; Huang, Y. C. J Appl Polym Sci 2007, 106, 1992.
24. Mohan, Y. M.; Lee, K.; Premkumar, T.; Geckeler, K. E. Polymer 2007, 48, 158.
25. Wang, C.; Flynn, N. T.; Langer, R. Mater Res Soc Symp Proc 2004, 820, R2.2.1.
26. Hon Ho, C.; Tobis, J.; Sprich, C.; Thomann, R.; Tiller, J. C. Adv Mater 2004, 16, 957.
27. Furno, F.; Morley, K. S.; Wong, B.; Sharp, B. L.; Arnold, P. L.; Howdle, S. M.; Bayston, R.; Brown, P. D.; Winship, P. D.; Reid, H. J. J Antimicrobiol Chem 2004, 54, 1019.
28. Murali Mohan, Y.; Premkumar, T.; Lee, K. J.; Geckeler, K. E. Macromol Rapid Commun 2006, 27, 1346.
29. Yang, T.-H. Recent Patents Mater Sci 2008, 1, 29.
30. Keshava Murthy, P. S.; Murali Mohan, Y.; Sreeramulu, J.; Mohana Raju, K. React Funct Polym 2006, 66, 1482.
31. Wang, C.; Flynn, N. T.; Langer, R. Adv Mater 2004, 16, 1074.
32. Vimala, K.; Samba Sivudu, K.; Murali Mohan, Y.; Sreedhar, B.; Mohana Raju, K. Carbohydr Polym 2009, 75, 463.
33. Saraydin, D.; Karadağ, E.; Güven, O. Polym Bull 1998, 41, 577.
34. Peniche, C.; Cohen, M. E.; Vazquez, B.; Roman, J. S. Polymer 1997, 38, 5977.
35. Saraydin, D.; Öztop, H. N.; Karadağ, E.; Çaldiran, Y.; Güven, O. Appl Bio Biotechnol 1999, 82, 115.
36. Karadağ, E.; Saraydin, D. Polym Bull 2002, 48, 299.
37. Porter, T. L.; Stewart, R.; Reed, J.; Morton, K. Sensors 2007, 7, 1980.